

Morphological and photosynthetic variations in the process of spermatia formation from vegetative cells in *Porphyra yezoensis* Ueda (Bangiales, Rhodophyta) and their responses to desiccation

Rui-Ling Yang · Wei Zhou · Song-Dong Shen ·
Guang-Ce Wang · Lin-Wen He · Guang-Hua Pan

Received: 15 May 2011 / Accepted: 4 November 2011 / Published online: 20 November 2011
© Springer-Verlag 2011

Abstract *Porphyra yezoensis* has a macroscopic foliage gametophyte phase with only a single cell layer, and is ideally suited for the study of the sexual differentiation process, from the vegetative cell to the spermatia. Firstly, we compared variations in the responses of the vegetative and male sectors to desiccation. Later, cell tracking experiments were carried out during the formation of spermatia from vegetative cells. The two sectors showed similar tolerance to desiccation, and the formation of spermatia from vegetative cells was independent of the degree of desiccation. Both light and scanning electron microscopy (SEM) observations of the differentiation process showed that the formation of spermatia could be divided into six phases: the one-cell, two-cell, four-cell, eight-cell, pre-release

and spermatia phases. Photomicrographs of Fluorescent Brightener staining showed that the released spermatia had no cell walls. Photosynthetic data showed that there was a significant rise in $Y(II)$ in the four-cell phase, indicating an increase in photosynthetic efficiency of PSII during this phase. We propose that this photosynthetic rise may be substantial and provide the increased energy needed for the formation and release of spermatia in *P. yezoensis*.

Keywords Desiccation-tolerant · Effective quantum yield · Electron transport rate · *Porphyra* · Sexual differentiation · Spermatia

Abbreviations

| | |
|---|---|
| APC | Allophycocyanin |
| CA | Carbonic anhydrase |
| Chl <i>a</i> | Chlorophyll <i>a</i> |
| DCMU | Diuron, 3-(3, 4-dichlorophenyl)-1, 1-dimethylurea |
| ETR(I) | Relative rates of photosynthetic electron transport of PSI |
| ETR(II) | Relative rates of photosynthetic electron transport of PSII |
| <i>F</i> | The current fluorescence yield |
| <i>F</i> ₀ | The intrinsic fluorescence |
| <i>F</i> _m | Maximum fluorescence yield |
| <i>F</i> _m ' | The maximum fluorescence yield in active radiation |
| <i>F</i> _v | Variable fluorescence yield |
| <i>F</i> _v / <i>F</i> _m | Optimum quantum yield of PSII |
| PAR | Photosynthetic active radiation |
| PC | Phycocyanin |
| PE | Phycocerythrin |
| PSI (II) | Photosystem I (II) |
| RWC | The relative water content |

R.-L. Yang and W. Zhou contributed equally to this publication.

R.-L. Yang · G.-H. Pan
College of Marine Science and Engineering,
Tianjin University of Science & Technology,
300457 Tianjin, China

W. Zhou · G.-C. Wang (✉) · L.-W. He
Key Laboratory of Experimental Marine Biology,
Institute of Oceanology, Chinese Academy of Sciences,
266071 Qingdao, China
e-mail: gcwang@qdio.ac.cn

W. Zhou · L.-W. He
Graduate School, The Chinese Academy of Sciences,
100039 Beijing, China

W. Zhou
Marine Fisheries Institute of Jiangsu,
226007 Nantong, China

S.-D. Shen
School of Life Science, Soochow University,
215123 Jiangsu, China

| | |
|---------------|---------------------------------|
| SEM | Scanning electron microscopy |
| <i>Y</i> | Effective quantum yield |
| <i>Y</i> (I) | Effective quantum yield of PSI |
| <i>Y</i> (II) | Effective quantum yield of PSII |

Introduction

The sexual differentiation process is an important step in development and the topic worth to study (Xu et al. 2002). Such study is facilitated through the choice of an experimentally suitable study species, and *Porphyra* sp. are amongst the best candidates in algae and higher plants (Kitade et al. 1998).

Porphyra is an economically important marine red alga and *Porphyra yezoensis* has become a model species for the study of marine plants. It is one of the most commonly cultivated species, and is grown widely in China, Japan, Korea and other Asian countries. *P. yezoensis* has a life history with macroscopic foliage, gametophyte phase and a microscopic filamentous, sporophyte phase, called the conchocelis (Candia et al. 1999; Nelson et al. 1999). The foliage phase of *P. yezoensis* generally has only a single cell layer and both, the male gametes and female gametes, appear in the same thallus, with the majority of the male gametes located on the margin of the thallus (Nelson et al. 1999).

Intertidal seaweed species experience alternate emersion and submersion as the tide comes in and out, resulting in a daily cycle of dehydration and re-hydration. Some species show particular tolerance to desiccation (Shafer et al. 2007; Gasulla et al. 2009), and can survive under dehydrating conditions. *Porphyra* are intertidal seaweeds and have specialized adaptations to prevent water loss. In aquaculture systems they are often artificially exposed to air to rid them of contamination by deleterious algae. Desiccation has little impact on the growth of *Porphyra*, further improving their suitability as a model species.

Although the vegetative cells of *P. yezoensis* are resistant to desiccation, there is little published information on the responses of their spermatia to desiccation, an important topic with regard to spermatia formation. To gain a more comprehensive understanding of the morphological and the physiological bases of male gametes differentiation from vegetative cells, we first determined the photosynthetic parameters of both the vegetative cells and male spermatangia mainly during the four-cell and following phases, and during dehydration and re-hydration. Second, because until recently there have been very few publications on *P. yezoensis*, especially with regard to the physiological characteristics of the sexual cells, we describe

both the morphological and some physiological characteristics of the process of vegetative cell differentiation into spermatia in *P. yezoensis*.

Chlorophyll fluorescence provides a swift, convenient and non-invasive method to assess algal physiology under different internal and external conditions and pulse amplitude-modulated (PAM) technology has been applied in this regard by an increasing number of researchers (Krause and Weis 1984; Lin et al. 2009a, b; Sussman et al. 2009; Gao et al. 2010). The microscopy-version of Imagine-PAM enables a single cell to be detected. Gao et al. (2010) applied Imagine-PAM to study changes in the photosynthetic properties of cells during sporangia formation and the development of spores of *Ulva prolifera*. The in vivo chlorophyll fluorescence yields of PS II (photosystem II) are determined using PAM fluorometry, and allow the calculation of photosynthetic parameters using established formulae (Schreiber 2004). *Y*(II) (effective quantum yield of PSII), the most useful parameter, is the quantum yield of PSII photochemistry, indicating the proportion of light absorbed by chlorophyll associated with the PSII used in photochemical processes. Another important parameter is *Fv/Fm*, which represents the potential (or maximum) quantum efficiency of PS II and is widely used as a sensitive indicator of photosynthetic performance (Maxwell and Johnson 2000). In this study, we applied Imagine-PAM to study the variations in photosynthesis during the differentiation process from vegetative cells to spermatia, in order to better understand the formation of spermatia in *P. yezoensis*.

Materials and methods

Sample cultivation

Thalli of *Porphyra yezoensis* were collected from Haian County, Jiangsu Province (32°38'N, 120°58'E), China, and cultured in natural seawater at 10°C, 40 $\mu\text{mol m}^{-2}\text{s}^{-1}$, 12L:12D. The water was changed every 2 days.

Measurement of carbonic anhydrase (CA) activity and pigment content of vegetative and spermatangial cells

According to the experimental design method of Wilbur and Anderson (1948), CA activity was determined with the following minor modification (Gómez-Pinchetti et al. 1992; Israel and Beer 1992; Szabo and Colman 2007): 0.1 g pieces of vegetative or spermatangial materials were suspended in 10 ml 20 mM sodium barbital buffer containing 400 mM K_2SO_4 (pH 8.3). The assay was started by the rapid addition of 5 ml of ice-cold CO_2 -saturated

distilled water into the buffer solution placed in ice water. The time required for a decrease in pH from 8.3 to 8.0 was recorded and CA activity was calculated following Wilbur and Anderson (1948). CA activity was calculated using a WA unit, which was defined as $(T_c/T_s)^{-1}$, where T_c and T_s represent the times of pH changes in the absence and presence of algal material, respectively (Gómez-Pinchetti et al. 1992; Israel and Beer 1992; Szabo and Colman 2007). Each sample experiment was replicated five times.

According to Kursar et al. (1983), phycobiliproteins were extracted from pigments by grinding 0.1 g pieces of fresh samples in liquid nitrogen, and transferred to a container with 4 ml distilled water and kept in the dark for 30 min at 4°C. The extraction mix containing proteins was then centrifuged at 8000 g for 10 min. The supernatant was decanted into a volumetric flask and metered to a volume of 5 ml with distilled water to determine the contents of phycobiliproteins. Chlorophyll *a* (Chl *a*) was extracted from the remaining precipitate by 90% (v/v) acetone in the dark for more than 24 h at 4°C (Kursar et al. 1983). The extraction containing Chl *a* was centrifuged at 8000 g for 10 min, decanted supernatant liquid to a 10 ml volumetric flask and added with 90% (v/v) acetone to a final volume of 10 ml. The absorbance of phycobiliproteins in the aqueous supernatants was recorded at 498.5, 614.0 and 651.0 nm, and their APC (allophycocyanin), PC (phycocyanin), and PE (phycoerythrin) contents were calculated following Kursar et al. (1983). The Chl *a* content was determined using a spectrophotometer under 664, 647 and 630 nm (Jeffrey and Humphrey 1975).

Measurement of water content of vegetative and spermatangial cells

Dehydration responses were evaluated by first gently removing excess water from the vegetative cells and spermatangia using filter paper. The samples were then placed on a culture dish and allowed to dry naturally at room temperature ($\sim 20^\circ\text{C}$) (Burrill et al. 2002; Shafer et al. 2007; Lin et al. 2009b). The relative water content (RWC) of a thallus was calculated according to the formula: $\text{RWC} = (W_t - W_d)/(W_0 - W_d) \times 100\%$, where W_t is the weight of the thallus subjected to desiccation treatment, W_d is the dry weight of the thallus after drying for about 24 h at 80°C, and W_0 is the wet weight of the hydrated thallus before desiccation.

Photosynthetic responses of vegetative and male spermatangial cells to dehydration and re-hydration

Photosynthetic measurement of both PSI (photosystem I) and PSII was carried out using a Dual-PAM-100 system (Heinz Walz, Effeltrich, Germany) and a fully computer-

controlled device for simultaneous assessment of P700 (PSI) and chlorophyll fluorescence (PSII) (Schreiber and Klughammer 2008). The photosynthetic parameters, $Y(\text{I})$ (effective quantum yield of PSI), $Y(\text{II})$ (effective quantum yield of PSII) and F_v/F_m (optimum quantum yield of PSII), of the two different segments were determined during both dehydration and re-hydration as described by Lin et al. (2009b). The thalli, including the vegetative and the male sectors, respectively, were DCMU (diuron, 3-(3, 4-dichlorophenyl)-1, 1-dimethylurea) treated by incubation in a 50 μM DCMU solution for 5 min. This process was repeated for three or more replicated pieces of each tissue.

The differentiation process from vegetative cells to spermatia

It was necessary to first become familiar with the types of cells found during the process of differentiation from vegetative cells into sexually mature male cells. This process could be divided into six phases; the one-cell, two-cell, four-cell, eight-cell, pre-release and spermatia phases.

Staining with Fluorescent Brightener

Fluorescent Brightener (F-3543 Sigma-Aldrich) was used in this study to detect the cell walls of the various cells. Tissues were stained with 0.01% Fluorescent Brightener (w/v) for 10 min and then washed three times with filtered seawater to remove the remnant dye (Fan et al. 2008). The fluorescence of the cell wall stained with Fluorescent Brightener was observed through a UV filter with an excitation wavelength of 340–380 nm using a fluorescence equipped Leica DM 2500 microscope. Photomicrographs of light and fluorescence images were taken in tiff format using the Leica Application Suite system.

Preparation for SEM (scanning electron microscopy)

Before fixation, the samples were washed carefully to remove any sand adhering to the surface. They were then fixed directly in phosphate-buffered saline (PBS) solution containing 5% (v/v) glutaraldehyde for 2 h at 4°C. The fixed samples were subsequently dehydrated in an ethanol gradient of 30, 50, and 70% for 15 min in turn.

Variation of photosynthetic activities of male sexual cells during the differentiation process

The chlorophyll fluorescence emission at each phase was measured using an Imaging-PAM (Heinz Walz) and the saturation pulse method. The thalli of *P. yezoensis* were kept in the dark for about 15 min before the experiment.

In the absence of actinic illumination, the minimal (F_0) and maximal (F_m) fluorescence yields of these dark-adapted thalli were induced using a measuring light and by the application of a saturation pulse light, respectively, and the optimal PSII quantum yield (F_v/F_m) was calculated. The maximum effective PSII quantum yield $Y(II)$ ($\Delta F/F_m' = (F_m' - F)/F_m'$) was determined according to the values of the current fluorescence yield (F) and the maximum fluorescence yield (F_m') of the light-adapted cells. The relative photosynthetic electron transport rate ($rETR = Y \cdot PAR \cdot 0.84 \cdot 0.5$) was calculated as the effective quantum yield (Y) multiplied with the photosynthetic active radiation (PAR) received by PS (Lin et al. 2009b).

Statistical analyses

Statistical analyses of the data were done according to Lin et al. (2009b). The data are mean values \pm SD obtained from more than three biological experiments. All comparisons between mean values were determined by Student's t test with 95% significance level ($P < 0.05$).

Results

Comparative analyses of CA activities and pigment content of the vegetative and the spermatangial segments

There was a significant difference ($P < 0.05$) between the CA activities of the two different types of cell (Fig. 1). While the male cells showed a low CA activity of 0.56, the CA activity of the vegetative cells was about 1.5 WA/g (FW, fresh weight), i.e. almost three times higher.

All of the phycobiliproteins and Chl a contents of the vegetative cells were significantly higher ($P < 0.01$) than

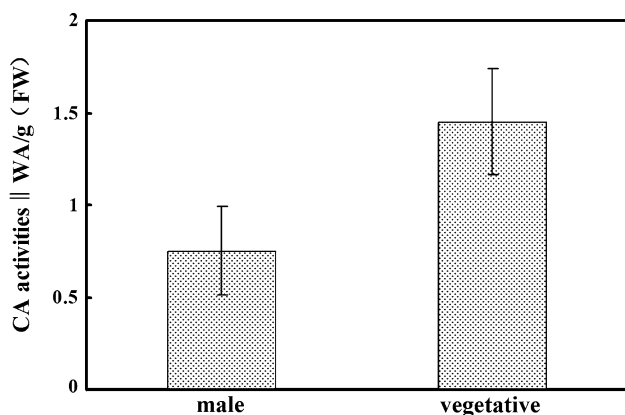


Fig. 1 Carbonic anhydrase activities of the vegetative cells and male cells of *P. yezoensis*. Data are the means of two independent experiments \pm SD

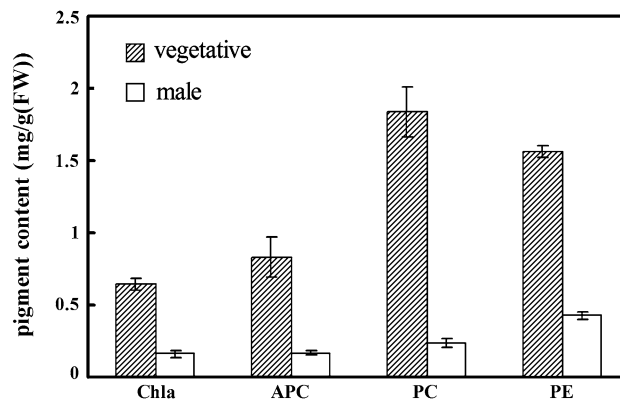


Fig. 2 Photosynthetic pigment analyses, including Chl a , APC, PC, and PE, of the vegetative cells and the male gametes of *P. yezoensis*. Data indicating the pigment content are the means \pm SD of 2 independent experiments

in the male cells (Fig. 2), and both types of cell had relatively higher contents of PC and PE compared with the other pigments. In addition, while PC was the most abundant pigment in the vegetative cells, PE was the most abundant pigment in the male cells.

Comparison of photosynthetic activity in the vegetative and male spermatangial cells in response to dehydration and re-hydration

The variance of the effective PSII quantum yield ($Y(II)$) of the vegetative and male tissues was broadly similar (Fig. 3). Both $Y(II)$ values declined but remained measurable as dehydration progressed, and reached their lowest level (around 0) at an RWC of 19%. During re-hydration, both values recovered to their initial levels after only 16 min. However, there were also some differences during the dehydration process: $Y(II)$ of the vegetative cells remained almost unchanged during the first phase of dehydration (up to RWC 76%), then started to decrease linearly during further dehydration (RWC 76–40%) before falling rapidly to a lower level at RWC 24%, and reaching its lowest point at RWC 19%. In contrast, the male sectors showed a much lower value of $Y(II)$. The $Y(II)$ of the male sectors was almost unchanged as the RWC declined from 100 to 49%, and declined in a linear fashion thereafter, with no strongly falling trend as seen in the vegetative cells. The maximum quantum yield (F_v/F_m) of the vegetative cells and male sectors (Fig. 3) showed a similar pattern during dehydration and re-hydration, except that the values for both sectors were still measurable at RWC 19% in dehydration, indicating the potential activation of the effective PSII quantum yield.

The variations in the effective PSI quantum yield $Y(I)$ of the vegetative cells and male sectors showed a similar tendency, except that $Y(I)$ of the male sectors was almost

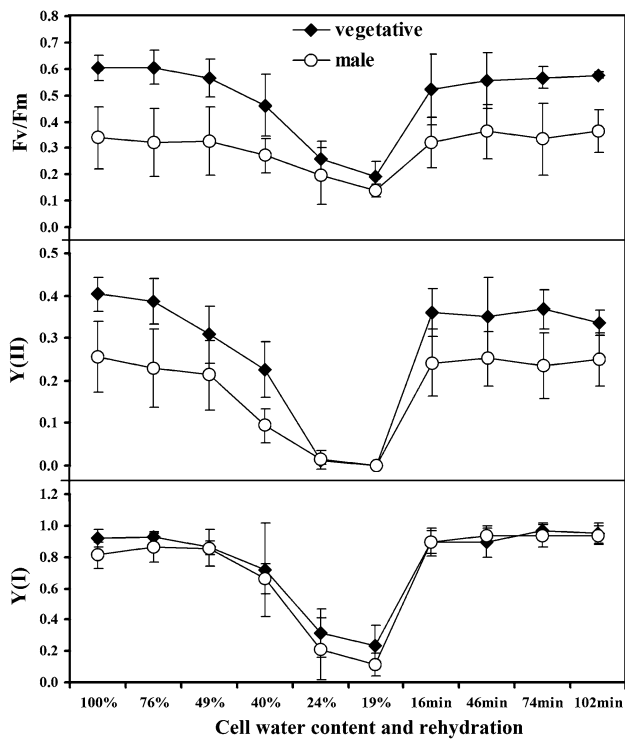


Fig. 3 Variation in the effective quantum yield of PSI, $Y(I)$, effective quantum yield ($Y(II)$), and maximum quantum yield (Fv/Fm) of PSII in the dehydration and re-hydration process in *P. yezoensis*. Data are mean values \pm SD from 4 to 12 biological replicates

equal to that of the vegetative cells (Fig. 3). Moreover, it is worth mentioning that $Y(I)$ values were still measurable in both sectors during the last two phases (RWC 24,19%), with $Y(I)$ of the vegetative cells a little higher than that of the male sectors.

In order to obtain a deeper understanding of the response variation of PSI, we also determined the photosynthetic parameters ETR(I) of the two sectors, treated with 50 μ M DCMU during the water content conditions. As shown in

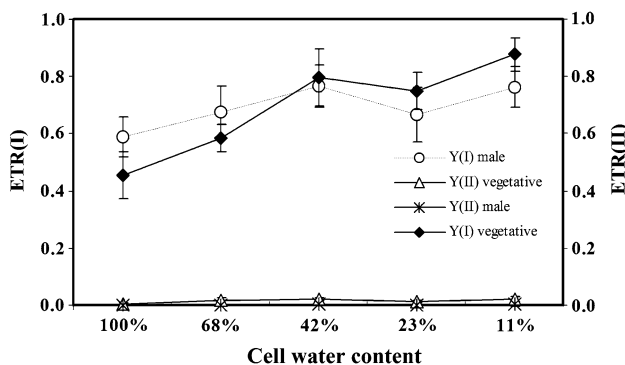


Fig. 4 Variation of electron transfer rate of PS(I), ETR(I) and of PS(II), ETR(II) treated with DCMU in the dehydration process of *P. yezoensis*. Data are the means \pm SD from 4 to 12 biological replicates

Fig. 4, the two sectors showed similar tendencies following treatment with DCMU. During desiccation, the ETR(I) of both the vegetative and the male spermatangial sectors remained stable at measurable values (Fig. 4). As Fig. 4 shows, the ETR(II) of both sectors were close to 0 at all of phases of dehydration, indicating that there was no electron transport in PSII.

Differentiation in the formation of spermatia from vegetative cells

Observation of cell walls

As shown in Fig. 5a–g, staining with the Fluorescent Brightener resulted in a light-blue fluorescence in all of the cell phases except the last. The vegetative cell walls were most easily stained, and their fluorescence was the brightest and clearest. However, clear staining was most difficult to obtain in cells from the later phases, such as the eight-cell phase, and no cell walls were detected in the released spermatia. The vegetative cells that differentiate into male gametes showed initial division into two cells of similar size. Subsequently these subcells became rounded and tended to distribute themselves equally in the tissues (Fig. 5a, b), indicating the beginning of their differentiation into spermatia. The size of the cells tended to be larger in the one-cell phase.

SEM observation of the cell surface

Figure 6 shows the surface characteristics of the cells in each phase during the differentiation process. The ridges on the cell surface are particularly noticeable (Fig. 6a–f), and generally became smaller and flatter during the transition from vegetative cells to the smaller spermatia cells. An exception was the rather bumpy cell surface in the pre-release phase, suggesting that these cells have rather thin envelopes. The spermatia themselves, however, had few ridges on the surface (Fig. 6g-1, g-2). Two smaller cells (labeled with short arrowheads) had a similar size to the vegetative cell (labeled with a long arrowhead) (Fig. 6a), consistent with the light- and fluorescence-photomicrograph images (Fig. 5a).

Photosynthetic parameters of PSII

The effective quantum yield ($Y(II)$) of PSII dropped slightly during the process of vegetative cell division at the two-cell phase. During the four-cell phase, however, the $Y(II)$ of the male cells increased significantly ($P < 0.05$), to a value of about 0.48, somewhat higher than that of the vegetative cells, before falling to 0 during the eight-cell and later phases (Fig. 7). The value of the maximal

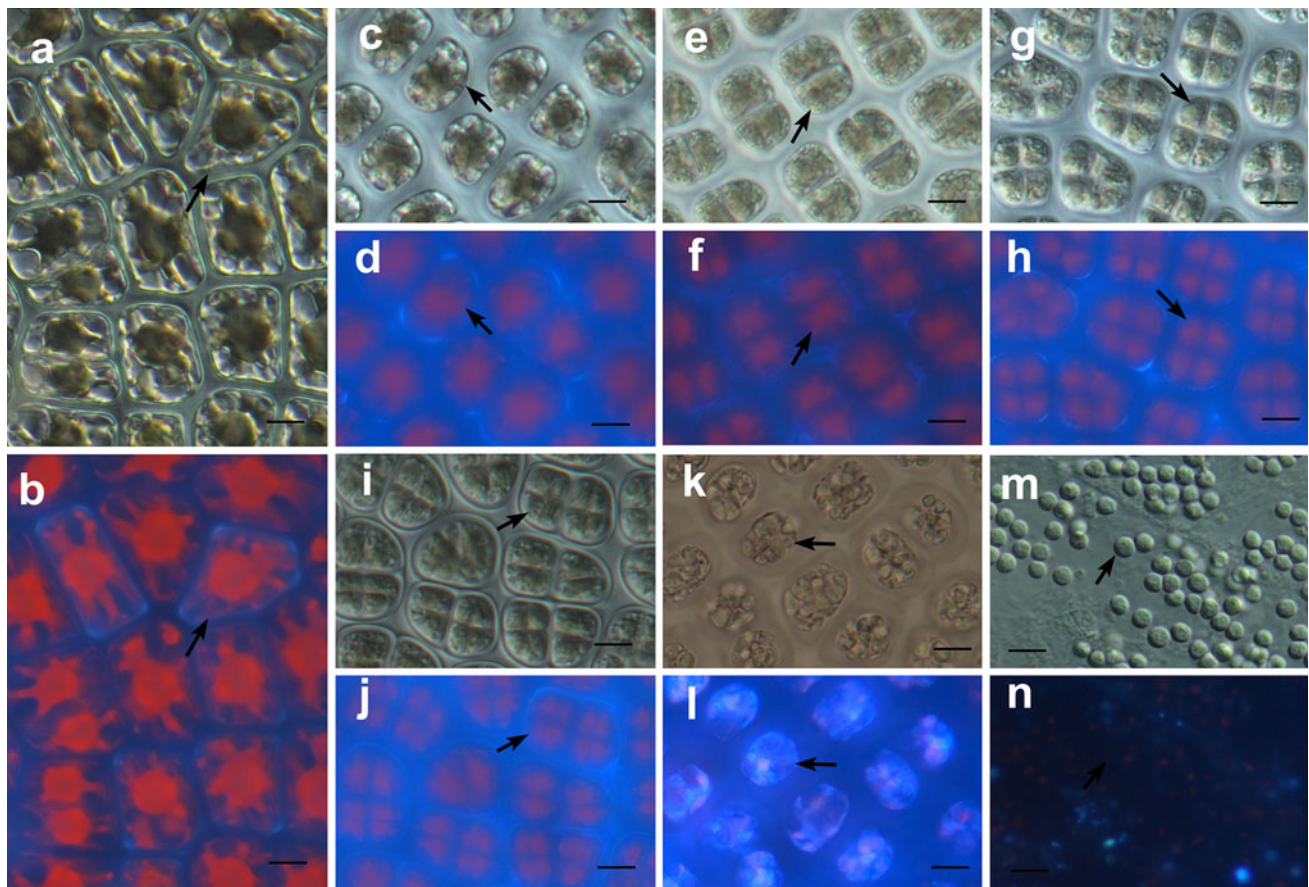


Fig. 5 **a, c, e, g, i, k, m** Light-microscopic images of cell walls during the differentiation process culminating in released sperm of *P. yezoensis*. **b, d, f, h, j, l, n** results with Fluorescent Brightener. **a, b** Vegetative cell, **c, d** One-cell stage (mother cell), **e, f**

stage, **g, h** Four-cell stage, **i, j** Eight-cell stage, **k, l** Pre-release cell and **m, n** Released sperms. The arrows mark a typical cell of the respective differentiation phase. Bar = 10 μ m

quantum yield (F_v/F_m) varied in a similar pattern to that of $Y(II)$, with a slight rise during each subsequent developmental phase (Fig. 7). However, the value of F_0 (the basic fluorescence) (Fig. 7) fell continuously from 0.06 in the vegetative cell phase to 0.01 in the pre-release phase. Microscopic observations tracking cell development from the vegetative to the pre-release phase showed that cells generally remained in each phase for about a day, except for the four-cell phase, in which they stayed for about 2 days.

Discussion

Resistance of desiccation by the male segment

CA plays an important role in photosynthesis, acting as an enzyme to catalyze the reversible conversion of CO_2 (Coleman 2000). Chlorophylls and biliproteins are well-known to function in harvesting light or transferring absorbed light (Van van Norman et al. 1948; Brody and

Emerson 1959; Kursar and Alberte 1983; Rowan 1989) and their concentration is related to photosynthetic efficiency (Yokoya et al. 2007). Our results show that CA activity and the amounts of both Chl *a* and phycobiliproteins are significantly higher ($P < 0.01$) in the vegetative segment than that in the spermatangial cells (Figs. 1, 2). It has been reported that higher photosynthetic pigment contents are correlated with higher photosynthetic activity in lower light conditions (Ramus et al. 1976; Stengel and Dring 1998; Han et al. 2003). Our desiccation experiment was carried out in weak scattered light and much higher values of $Y(II)$ and F_v/F_m were observed in the vegetative cell at RWC 100% (Fig. 3). These results were well correlated with the higher CA activity and the higher pigment contents of the vegetative cell in *P. yezoensis* (Fig. 1). Therefore, we speculate that higher CA activity and pigment contents may be one of the reasons for the higher photosynthetic activity in the vegetative cells in *P. yezoensis*. To sum up, we conclude that the photosynthetic activity of the vegetative cells in *P. yezoensis* is higher than that of the male cells.

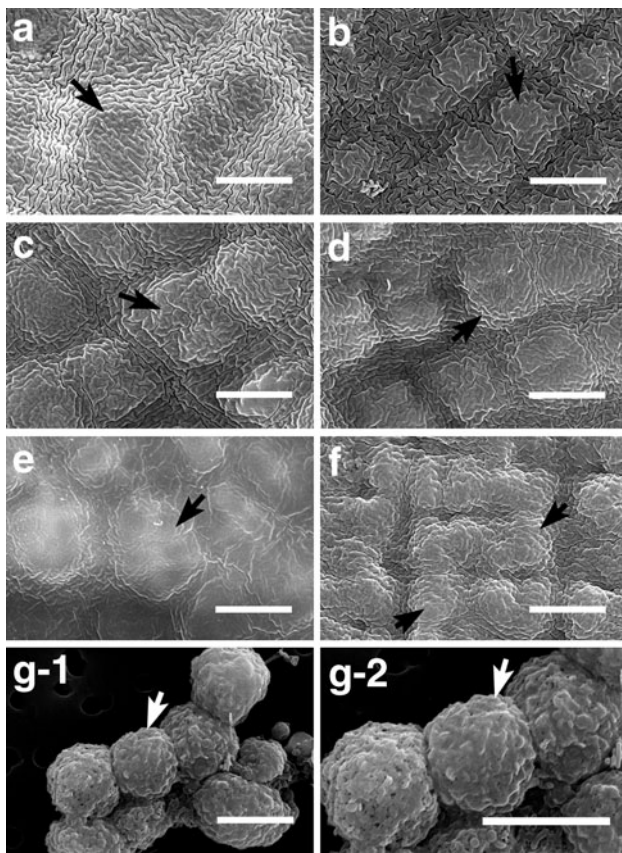


Fig. 6 SEM pictures of the cell surface of *P. yezoensis*. **a–g** Vegetative cell, one-cell, two-cell, four-cell, eight-cell, pre-release and sperm phase, respectively. The *arrows* mark a typical cell of the respective differentiation phase. *Bar* = 10 μ m

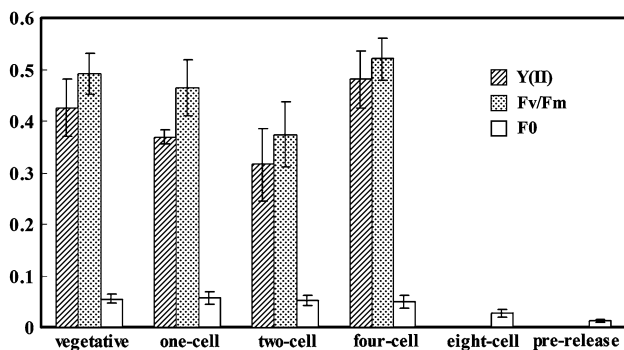


Fig. 7 Variation in the effective quantum yield ($Y(II)$), the maximum quantum yield (Fv/Fm), and the intrinsic fluorescence yields $F0$ of PSII during the differentiation process before sperm release in *P. yezoensis*. Data are the means from 4 to 12 biological replicates

Water deficit is the most important factor restricting the development of photosynthetic organisms (Yokoya et al. 2007) and the distributions of plants are well correlated with the ability of various species to deal with prevailing water stresses (Smith and Berry 1986; Burritt et al. 2002). In this study, photosynthetic activity in the vegetative

segment of *P. yezoensis* was reduced in response to desiccation, as indicated by a fall in $Y(II)$ and $Y(I)$ (Fig. 3). When submerged in water, the vegetative segment was able to recover photosynthetic capacity (Fig. 3). Recent studies have demonstrated the inactivity of PSII (Heber et al. 2000, 2006, 2010; Heber 2008) and blockage of electron transport through PSI as a result of desiccation (Chen and Hsu 1995) and the recovery of photosynthesis after re-hydration (Heber 2008). It is worth mentioning that $Y(I)$ of the vegetative segment remained positive during the dehydration process while $Y(II)$ dropped to 0 when RWC reached 19% (Fig. 3). Moreover, the results from the DCMU treated tissues showed that ETR(I) response to desiccation of the vegetative cell was still measurable at an RWC of 11% (Fig. 4). These results are in accord with those of Lin et al. (2009b) who showed that the photosynthetic capacity of *P. katadai* depended on the accommodative ability of PSI under conditions of severe dehydration. It has been suggested that desiccation may disrupt the transfer of energy from antenna pigments to the PSII reaction (Smith et al. 1986; Davison and Pearson 1996; Heber et al. 2000) and that there is a transfer of excitation energy away from PSII to PSI, where it appears to be dissipated as heat associated with cyclic PSI electron transport, and to assist in the survival of desiccation (Öquist and Fork 1982; Fork et al. 1986; Davison and Pearson 1996; Heber et al. 2000). Moreover, Jacob et al. (1992) reported that the green alga *Prasiola crispa* ssp. *antarctica* (Kütz.) Knebel could resist desiccation, and that the absence of vacuoles appears to be an essential prerequisite for the ability to survive periods of desiccation. Since there is also no vacuole in *Porphyra*, perhaps the absence of vacuoles is another explanation for the desiccation tolerance of *P. yezoensis*. We further conclude, therefore, that the vegetative sector of *P. yezoensis* perhaps resists desiccation through an activation of PSI.

Although the $Y(II)$ of the male cells of *P. yezoensis* evidently respond to desiccation less well than the vegetative cells, the $Y(I)$ and ETR(I) responses to desiccation were similar to those of the vegetative cells both in the absence and presence of DCMU (Figs. 3 and 4). We therefore conclude that in *P. yezoensis*, the male cells can also resist desiccation by maintaining activation of PSI, just like the vegetative cells, allowing the development from vegetative cells to the spermatia without regard for the state of hydration.

The rise in photosynthetic capacity in the four-cell phase may provide the increased energy needed for the development of the male gametophyte

As shown in Figs. 5 and 6, the light-microscope images were well correlated with the SEM observations of the surface characteristics in the different cell phases during

the spermatia formation process in *P. yezoensis*. The cell wall of the vegetative cells of *P. yezoensis* resisted staining and most ridges on the cell surfaces became smaller and flatter during the process of differentiation into a sperm cell, indicating that the cell wall becomes thinner as the differentiation process progresses. The tendency for cell size to increase may be evidence that the wall surrounding the newly formed spermatia in *P. yezoensis* is an extension of the spermatangial mother cell wall (Kugrens 1974; Kim and Fritz 1993; Delivopoulos 2000). The cell walls appear to become thinner, and the cell surface flatter as the differentiation process progresses (Figs. 5 and 6). Hawkes (1978) mentioned that at the time of release there is no cell wall around the spermatium in *P. gardneri*, consistent with this study.

This study represents the first photosynthetic analysis of the spermatogenesis of *P. yezoensis*, including the vegetative cell and all the stages of spermatia differentiation throughout this developmental process. Interestingly, the most important feature of the photosynthesis of spermatangia is that there was a rise in $Y(II)$ ($P < 0.05$) during the four-cell phase (Fig. 7), indicating an increase in the photosynthetic efficiency of PSII. Although no studies on photosynthesis of spermatogenesis are available for *Porphyra*, early investigations showed that the maturation of tetraspores was signaled by the presence of abundant starch granules at the last developmental stage during tetrasporogenesis in a marine red algae *Rhodymenia californica* var. *attenuata* (Delivopoulos 2002, 2004). Furthermore, in higher plants, the development and germination of pollen requires high-energy expenditure. Aerobic fermentation takes place concurrently with respiration at a high rate of sugar metabolism during pollen development and germination in tobacco, as a result of the increased demand for energy and biosynthetic intermediates (Bucher et al. 1995; Tadege and Kuhlemeier 1997). The typically trinucleate pollen of *Aster tripolium* L. respired at a high rate, maintaining a high energy charge, their mitochondria reached maximum electron-transducing capacity within 2 min of incubation, and pollen tube growth started within 3 min (Hoekstra 1979). In *Lilium* cultivars, starch in the anther cell layers was partly consumed during the growth phase of pollen development (Clément et al. 1994). In this regard, we propose that the rise in photosynthesis at the four-cell stage may provide the increased energy needed by the spermatangial development and the release of the mature spermatia.

Mature released sperm usually lack chloroplasts (Wang and Xu 1984; Delivopoulos 2000) and starch grains (Wang and Xu 1984), perhaps indicating that no distinct photosynthetic activity occurs, as suggested by the lack of a measurable value of $Y(II)$ or F_v/F_m , at the eight-cell and pre-release stages in PSII.

The parameter F_0 , indicating the level of intrinsic fluorescence, is comparable to the level of Chl *a* content. The continuous reduction observed in F_0 (Fig. 7) accords with our morphological observations, in which the color stain became much weaker during the later stages of the differentiation process.

Acknowledgments This work was supported by the National Natural Science Foundation of China (No. 30830015, 40806063, 41176134, 30970302, 41106131, 41176137).

References

- Brody M, Emerson R (1959) The quantum yield of photosynthesis in *Porphyridium cruentum*, and the role of chlorophyll *a* in the photosynthesis of red algae. *J Gen Physiol* 43:251–264
- Bucher M, Brander KA, Sbicego S, Mandel T, Kuhlemeier C (1995) Aerobic fermentation in tobacco pollen. *Plant Mol Biol* 28:739–750
- Burritt DJ, Larkindale J, Hurd CL (2002) Antioxidant metabolism in the intertidal red seaweed *Stictosiphonia arbuscula* following desiccation. *Planta* 215:829–838
- Candia A, Lindstrom S, Reyes E (1999) *Porphyra* sp. (Bangiales, Rhodophyta): reproduction and life form. *Hydrobiologia* 398(399):115–119
- Chen YH, Hsu BD (1995) Effects of dehydration on the electron transport of *Chlorella*. An in vivo fluorescence study. *Photosynth Res* 46:295–299
- Clément C, Chavant L, Burrus M, Audran JC (1994) Anther starch variations in *Lilium* during pollen development. *Sex Plant Reprod* 7:347–356
- Coleman JR (2000) Carbonic anhydrase and its role in photosynthesis. In: Leegood RC, Sharkey TD, Von Caemmerer S (eds) *Advances in photosynthesis*, vol 9: photosynthesis: physiology and metabolism. Kluwer Academic Publisher, Dordrecht, pp 353–367
- Davison IR, Pearson GA (1996) Stress tolerance in intertidal seaweeds. *J Phycol* 32:197–211
- Delivopoulos SG (2000) Ultrastructure of spermatogenesis in the red alga *Osmundea spectabilis* var. *spectabilis* (Rhodomelaceae, Ceramiales, Rhodophyta). *Phycologia* 39:517–526
- Delivopoulos SG (2002) Ultrastructure of tetrasporogenesis in the red alga *Osmundea spectabilis* var. *spectabilis* (Rhodomelaceae: Ceramiales: Rhodophyta). *Mar Biol* 140:921–934
- Delivopoulos SG (2004) Ultrastructure of tetrasporogenesis in the red alga *Rhodymenia californica* var. *attenuata* (Rhodymeniaceae, Rhodymeniales, Rhodophyta). *Bot Mar* 47:222–230
- Fan XL, Wang GC, Li DM, Xu P, Shen SD (2008) Study on early-stage development of conchospore in *Porphyra yezoensis* Ueda. *Aquaculture* 278:143–149
- Fork DC, Bose S, Herbert SK (1986) Radiationless transitions as a protection mechanism against photoinhibition in higher plants and a red alga. *Photosynth Res* 10:327–333
- Gao S, Chen XY, Yi QQ, Wang GC, Pan GH, Lin AP, Peng G (2010) A strategy for the proliferation of *Ulva prolifera*, main causative species of green tides, with formation of sporangia by fragmentation. *PLoS ONE* 5:e8571
- Gasulla F, Gómez de Nova P, Esteban-Carrasco A, Zapata JM, Barreno E, Guéra A (2009) Dehydration rate and time of desiccation affect recovery of the lichenic algae *Trebouxia erici*: alternative and classical protective mechanisms. *Planta* 231:195–208
- Gómez-Pinchetti JL, Ramazanov Z, García-Reina G (1992) Effect of inhibitors of carbonic anhydrase activity on photosynthesis in the

- red alga *Soliera filiformis* (Gigartinales: Rhodophyta). *Mar Biol* 114:335–339
- Han T, Han Y, Kain JM, Häder D (2003) Thallus differentiation of photosynthesis, growth, reproduction, and UV-B sensitivity in the green alga *Ulva pertusa* (Chlorophyceae). *J Phycol* 39:712–721
- Hawkes MW (1978) Sexual reproduction in *Porphyra gardneri* (Smith et Hollenberg) Hawkes (Bangiales, Rhodophyta). *Phycologia* 17:329–353
- Heber U (2008) Photoprotection of green plants: a mechanism of ultra-fast thermal energy dissipation in desiccated lichens. *Planta* 228:641–650
- Heber U, Bilger W, Bligny R, Lange OL (2000) Phototolerance of lichens, mosses and higher plants in an alpine environment: analysis of photoreactions. *Planta* 211:770–780
- Heber U, Bilger W, Shuvalov VA (2006) Thermal energy dissipation in reaction centres and in the antenna of photosystem II protects desiccated poikilohydric mosses against photo-oxidation. *J Exp Bot* 57:2993–3006
- Heber U, Bilger W, Türk R, Lange OL (2010) Photoprotection of reaction centres in photosynthetic organisms: mechanisms of thermal energy dissipation in desiccated thalli of the lichen *Lobaria pulmonaria*. *New Phytol* 185:459–470
- Hoekstra FA (1979) Mitochondrial development and activity of binucleate and trinucleate pollen during germination in vitro. *Planta* 145:25–36
- Israel A, Beer S (1992) Photosynthetic carbon acquisition in the red alga *Gracilaria conferta*. II. Rubisco carboxylase kinetics, carbonic anhydrase and HCO₃⁻ uptake. *Mar Biol* 112:697–700
- Jacob A, Wiencke C, Lehmann H, Kirst GO (1992) Physiology and ultrastructure of desiccation in the green alga *Prasiola crispa* from Antarctica. *Bot Mar* 35:297–304
- Jeffrey SW, Humphrey GF (1975) New spectrophotometric equations for determining chlorophylls *a*, *b*, *c*₁ and *c*₂ in higher plants, algae, and natural phytoplankton. *Biochem Physiol Pflanzen* 167:191–194
- Kim GH, Fritz L (1993) Ultrastructure and cytochemistry of early spermatangial development in *Antithamnion nipponicum* (Ceramiaceae, Rhodophyta). *J Phycol* 29:797–805
- Kitade Y, Taguchi G, Shin JA, Saga N (1998) *Porphyra* monospore system (Bangiales, Rhodophyta): a model for the developmental biology of marine plants. *Phycol Res* 46:17–20
- Krause GH, Weis E (1984) Chlorophyll fluorescence as a tool in plant physiology. II. Interpretation of fluorescence signals. *Photosynth Res* 5:139–157
- Kugrens P (1974) Light and electron microscopic studies of the development and liberation of *Lancezowskia gardneri* Setch. Spermatia (Rhodophyta). *Phycologia* 13:295–306
- Kursar TA, Alberte RS (1983) Photosynthetic unit organization in a red alga. Relationships between light harvesting pigments and reaction centers. *Plant Physiol* 72:409–414
- Kursar TA, Vander MJ, Alberte RS (1983) Light-harvesting system of the red alga *Gracilaria tikvahiae*. I. Biochemical analysis of pigment mutations. *Plant Physiol* 73:353–360
- Lin AP, Wang C, Qiao HJ, Pan GH, Wang GC, Song LY, Wang ZY, Sun S, Zhou BC (2009a) Study on the photosynthetic performances of *Enteromorpha prolifera* collected from the surface and bottom of the sea of Qingdao sea area. *Chin Sci Bull* 54:399–404
- Lin AP, Wang GC, Yang F, Pan GH (2009b) Photosynthetic parameters of sexually different parts of *Porphyra katadai* var. hemiphylla (Bangiales, Rhodophyta) during dehydration and re-hydration. *Planta* 229:803–810
- Maxwell K, Johnson GN (2000) Chlorophyll fluorescence—a practical guide. *J Exp Bot* 51:659–668
- Nelson WA, Brodie J, Guiry MD (1999) Terminology used to describe reproduction and life history stages in the genus *Porphyra* (Bangiales, Rhodophyta). *J Appl Phycol* 11:407–410
- Öquist G, Fork DC (1982) Effects of desiccation on the excitation energy distribution from phycoerythrin to the two photosystems the red alga *Porphyra perforata*. *Physiol Plant* 56:56–62
- Ramus J, Beale SI, Mauzerall D (1976) Correlation of changes in pigment content with photosynthetic capacity of seaweeds as a function of water depth. *Mar Biol* 37:231–238
- Rowan KS (1989) Photosynthetic pigments of algae. Cambridge University Press, Cambridge
- Schreiber U (2004) Pulse-Amplitude-Modulation (PAM) fluorometry and saturation pulse method: an overview. In: Papageorgiou GC, Govindjee (eds) Chlorophyll fluorescence: a signature of photosynthesis. Springer, New York, pp 279–319
- Schreiber U, Klughammer C (2008) Saturation pulse method for assessment of energy conversion in PS I. *PAM Appl Notes* 1:11–14
- Shafer DJ, Sherman TD, Wyllie-Echeverria S (2007) Do desiccation tolerances control the vertical distribution of intertidal seagrasses? *Aquat Bot* 87:161–166
- Smith CM, Berry JA (1986) Recovery of photosynthesis after exposure of intertidal algae to osmotic and temperature stress: comparative studies of species with differing distributional limits. *Oecologia* 70:6–12
- Smith CM, Satoh K, Fork DC (1986) The effects of osmotic tissue dehydration and air drying on morphology and energy transfer in two species of *Porphyra*. *Plant Physiol* 80:843–847
- Stengel DB, Dring MJ (1998) Seasonal variation in the pigment content and photosynthesis of different thallus regions of *Ascophyllum nodosum* (Fucales, Phaeophyta) in relation to position in the canopy. *Phycologia* 37:259–268
- Sussman M, Mieog JC, Doyle J, Victor S, Willis BL, Bourne DG (2009) Vibrio zinc-metalloprotease causes photoinactivation of coral endosymbionts and coral tissue lesions. *PLoS ONE* 4:e4511
- Szabo E, Colman B (2007) Isolation and characterization of carbonic anhydrases from the marine diatom *Phaeodactylum tricorutum*. *Physiol Plant* 129:484–492
- Tadege M, Kuhlemeier C (1997) Aerobic fermentation during tobacco pollen development. *Plant Mol Biol* 35:343–354
- Van van Norman RW, French CS, Macdowall FDH (1948) The absorption and fluorescence spectra of two red marine algae. *Plant Physiol* 23:455–466
- Wang SJ, Xu ZD (1984) Ultrastructural studies on the reproductive organs of *Porphyra haitanensis* T. J. Chang et B. F. Zheng. *Hydrobiologia* 116/117:213–217
- Wilbur KM, Anderson NG (1948) Electrometric and colorimetric determination of carbonic anhydrase. *J Biol Chem* 176:147–154
- Xu HP, Weterings K, Vriezen W, Feron R, Xue YB, Derksen J, Mariani C (2002) Isolation and characterization of male-germ-cell transcripts in *Nicotiana tabacum*. *Sex Plant Reprod* 14:339–346
- Yokoya NS, Necchi O, Martins AP, Gonzalez SF, Plastino EM (2007) Growth responses and photosynthetic characteristics of wild and phycoerythrin-deficient strains of *Hypnea musciformis* (Rhodophyta). *J Appl Phycol* 19:197–205